ELSEVIER

The Reflectance Spectra of Organic Matter in the Visible Near-Infrared and Short Wave Infrared Region (400–2500 nm) during a Controlled Decomposition Process

E. Ben-Dor, Y. Inbar,† and Y. Chen‡*

The reflectance spectra of organic matter in the VIS-NIR-SWIR regions (400–2500 nm) were investigated with regard to possible changes that might occur during a biological decomposition process. Two different groups of organic matter were used in this study: a grape marc (CGM) and a separated cattle manure (CSM) that simulated pure organic matter endmembers in soils. Exposing the two materials for different decomposition durations (0–378 days) visually yielded color sequences as the compost aged. Significant changes in the reflectance spectra of both materials were also observed during the composting period, which provided parameters for controlling the composting process. The slopes in the VIS-NIR region were found to be basic parameters for monitoring changes and were found to be highly correlated with other chemical parameters often used for assessing organic matter conditions in the field (such as the C/N ratio). It was found that during the initial composting stage (0–60 days) the slope parameters were strongly affected by the decomposition activity and, hence, errors in the assessment of organic matter content of soils using slope (or band ratio) parameters are likely. Careful observation of the major spectral features reveals that the reflectance spectrum in the VIS-NIR-SWIR region is a very sensitive tool for monitoring slight changes. Application of the near-infrared analysis (NIRA) pathways revealed that OH and C—H groups combined with hygroscopic water, starch, cellulose, and lignin are the components having the highest correlations with composting time within the conditions used. Because of the small number of samples in each testing group a complete NIRA employing validation tests could not be carried out. We concluded that the reflectance spectrum in the VIS-NIR-SWIR region is a promising tool for monitoring the composting process and that the composting process may provide invaluable spectral information about soil organic matter during its biochemical degradation. ©*Elsevier Science Inc., 1997*

INTRODUCTION

Quantitative analysis of the Earth's surface from a distance has become a feasible task since vehicles such as imaging spectroscopy (IS) have entered the field of remote sensing. The IS sensors [e.g., Airborne Visible/Infrared Imaging Spectrometer (AVIRIS) (Vane et al., 1993), Geophysical Environment Research Imaging Spectrometer (GERIS) (Chang et al., 1994), and Multispectral Infrared and Visible Imaging Spectrometer (MIVIS) (Stanich and Osterwisch, 1994)], which are mounted onboard aircraft are able to provide near laboratory quality spectra of every ground pixel taken from altitudes up to 60,000 ft. The IS sensors usually cover the visible (VIS), near-infrared (NIR), and short-wave infrared (SWIR) regions (400–2500 nm) and recently have even extended into the IR spectral regions (2500–12,300 nm) (e.g., in MIVIS and GERIS). These regions consist of invaluable diagnostic information about many of the Earth's materials and enable the quantitative detection of the Earth's surface by taking full advantage of the contiguous spectrum provided by the IS sensors (e.g., Boardman and Kruse, 1994; Ben-Dor and Kruse, 1995).

* Department of Geography, Tel-Aviv University, Tel-Aviv, Israel
† Ministry of Environment, Jerusalem, Israel
‡ Department of Soil and Water Sciences, Faculty of Agriculture, The Hebrew University of Jerusalem, Israel

Address correspondence to Eyal Ben-Dor, Dept. of Geography, Tel-Aviv Univ., Ramat-Aviv, P.O. Box 39040, Tel-Aviv 66978, Israel.
Received 27 September 1995; revised 12 May 1996.

REMOTE SENS. ENVIRON. 61:1–15 (1997)

655 Avenue of the Americas, New York, NY 10010

0034-4257/97/$17.00
PII S0034-4257(96)00120-4

A priori knowledge of the spectral characteristics of all sensed objects is a primary condition for successful applications of any quantitative analysis. Many spectral libraries of rocks, minerals, and soils are available for that purpose (e.g., Stoner et al., 1980; Grove et al., 1992; Kruse and Hauff, 1992) and are widely used by many workers in the remote sensing field. A lack of similar libraries for leaf litter materials prompted Elvidge (1990) to create a spectral data base of nongreen components of many plant canopy species and their basic pure components. Although the chemistry of rocks, minerals and soils is thought to remain constant over time (i.e., years), organic matter in soils is not always stable, and its dynamics are strongly associated with factors that vary over time (Parton et al., 1994). Consequently, every organic matter spectra (e.g., fresh, dry, or decomposed litter) should be judged using the time factor as was introduced by McLellan et al. (1991a) using a wide range of litter age spectra in the 1100–2500 nm region.

In studies that have used reflectance spectra to assess soil organic matter (e.g., Kristof et al., 1971; Al-Abbas, 1972; Vinogradov, 1981), only minor consideration has been given to the organic matter dynamics of the soils, and detailed "spectral-based" information about the relationship between soil organic matter from various organic sources and their aging is still lacking. In recent limited studies, however, more consideration has been given to the above issue, (Aber et al., 1990; McLellan et al., 1991b), especially for leaf and litter materials. However, long periods of decomposition time (years), combined with the requirement of close field control during that time, render such examinations impractical and complicated.

Soil organic matter is a mixture of dead tissues of plants, animals, and secretion substances of organic organisms in various stages of degradation ("maturity"). The sequence of organic matter decomposition in soils is strongly determined by the soil's microorganism activity, which uses the fresh organic matter as an available energy source in a time domain. The young stage in the organic matter decomposition process refers to the initial phase of the microorganic activity, where no marginal changes occur within the chemistry of the parent organic material. The mature stage refers to the final stage of microorganic activity, where new complex compounds, often called humus, are formed (Inbar et al., 1989).

In the agriculture field, a process for rapidly decomposing fresh organic matter into humus is available for commercial purposes (Inbar et al., 1988). The process, termed "composting," uses controlled conditions, particularly moisture and aeration, to yield temperatures favorable for thermophilic microorganisms, to decompose the organic substrate into stabilized organic matter via production of CO_2, water, and minerals. The organic matter undergoes an initial, rapid stage of decomposition, and then is in the process of humificiation (Zucconi and Bertoldi, 1987). Usually such a process takes weeks and works very well on various fresh organic matter compounds used as substrates. The ability of the composting process to work under an ideal controlled environment makes it a tool for rapidly studying and monitoring the decomposition process under "laboratory" conditions.

In this study we employed a composting process on two nonlitter organic matter components and carefully checked their products chemically and spectrally on a routine basis. The primary goals of this article are to report the results of the above systematic study, to find spectral parameters for assessing the organic matter maturity, and to examine the possibility of using the composting process as a method of creating a spectra base library of aging organic matter.

MATERIALS AND METHODS

Two basic organic materials were used as follows:

1. CGM: Grape marc, which consists of grape skins and seeds that are left over after wine grape processing. It was composted without additives in windrows for 378 days. The 30 m^3 heap was turned, mixed thoroughly, and sampled after 0 days, 7 days, 13 days, 33 days, 57 days, 86 days, 160 days, and 378 days. Water was added to the pile whenever the moisture level dropped below 50%. Samples were stored at −4°C. Two-liter subsamples were taken, dried at 105°C, ground to pass through a 0.25-mm sieve, and stored in a desiccator under vacuum.
2. CSM: A solid fibrous fraction ("cake") that was obtained from liquid cattle manure was composted in two 1 m^3 perforated plastic boxes for a period of 147 days. The material was turned, mixed thoroughly and sampled after 3 days, 10 days, 18 days, 26 days, 39 days, 60 days, 91 days, 116 days, and 147 days. Samples were stored at −4°C. Subsamples were taken, dried at 105°C, ground to pass through a 0.255-mm sieve, and stored in a desiccator under vacuum.

For all spectroscopic measurements, the samples were exposed to room atmosphere for about 14 days and then spectrally measured as described below:

Spectral Measurements and Manipulation

Spectral measurements: The spectral reflectance of the organic matter powder was recorded using double beams of the Cary UV-VIS-NIR spectrophotometer Model 5E of Varian, Inc. The spectrometer was optimized to the VIS-NIR-SWIR region (400–2500 nm), had a constant spectral resolution of 1 nm, and yielded 2100 spectral bands.

The diffuse reflectance was measured by a Diffuse Reflectance Accessory (DRA) Labsphere integrating sphere

Table 1. The Color Values of the Dry Materials (SGM and CSM), as Determined by Using the Munsel Color Chart (Munsel Color, 1975)

Sample Symbol	*Compost Time (days)*	*Munsel Parameter*		
		Hue	*Value/Croma*	*Color Name*
CGM				
00	0	2.5YR	3/3	Dark reddish brown
0	7	2.5YR	2/3	Very dark reddish brown
I	13	5YR	3/4	Brownish black
II	33	5YR	2/4	Very dark reddish brown
III	57	7.5YR	2/2	Brownish black
IV	86	5YR	2/1	Brownish black
V	160	7.5YR	2/2	Brownish black
VI	378	7.5YR	1.7/1	Black
CSM				
I	3	2.5YR	5/4	Yellowish brown
II	10	2.5YR	5/3	Yellowish brown
III	18	10YR	4/3	Dull yellowish brown
IV	26	10YR	3/2	Brownish black
V	39	7.5YR	3/2	Brownish black
VI	60	7.5YR	3/4	Dark brown
VII	91	7.5YR	3/3	Dark brown
VIII	116	5YR	2/1	Brownish black
IX	147	5YR	2/3	Very dark reddish brown

(Model RSA-CA-50D), coated with polytetrafluoroethylene (PTFE) ("halon"). The powders of the organic matters were packed into black stainless steel sample holders using a standard sample preparation procedure. The reflectance was reported relative to a PTFE standard spectrum, and was recorded under similar spectroscopic and geometric conditions of the samples.

RESULTS AND DISCUSSION

Figures 1 and 2 present the reflectance spectra of CGM and CSM, respectively, and the exact position of significant spectral features that were directly extracted from these figures. Each figure represents two extremes of the composting stages, termed "young" (t_0=0 days for CGM and t_1=3 days for CSM, respectively) and "mature" (t_8=378 days for CGM and t_9=147 days for CSM, respectively). Also provided in the small box of each figure are the spectra for all the composition stages of the two materials. For both materials, throughout all stages (young through mature) spectral changes can be seen in three areas: 1) decreasing baseline height ("albedo"), 2) decreasing baseline slope, and 3) changes in the spectral features (position and intensity).

Changes in the Baseline

In Table 1 we summarized the color values of both the CGM and the CSM materials as determined by using Munsel color parameters (Munsel Color, 1975). Table 1 shows a significant hue sequence in both materials changing from light in the young to dark in the mature stages. The corresponding spectra in Figures 1 and 2 show a baseline sequence [albedo (height) and slope] in both materials that changes from high albedo and sharp slope for the young stages, to low albedo and moderate slope for the mature stages. Color observation is a basic vehicle for judging the organic matter condition (Leger et al., 1979) and is often used as a rule of thumb in the field to assess organic matter content (Buol et al., 1973; Krishnan et al., 1981). Based on the spectral information associated with the VIS-NIR spectral region and color, we generated a spectral parameter in order to better assess the visible changes as follows: I) the slope between 638 nm and 450 nm and II) the slope between 800 nm and 680 nm.

In Figures 3a and 3b the two above-mentioned slopes are plotted against the composting time for all the CGM and the CSM samples. It can be observed that for a given (composting) time, the slope II values are higher than the slope I values (except in the "mature" stage). In general, for both slopes (I and II) a decay like function can be observed in both CGM and CSM materials. This trend is highly (negative) correlated with other chemical changes reported by Inbar et al. (1991) and Chen and Inbar (1994) for the same population such as: cation exchange capacity (CEC), humification parameters, and carbon to nitrogen ratio (C/N). For dry plant materials, Elvidge (1990) addressed the "visible wing" (and, hence, the slope parameter in this region) to the intense blue and ultraviolet absorptions in components such as lignin, tannins, and pectin. The decrease of the slope parameters during aging may, thus, represent a decrease in the above components' absorption and hence their concentration.

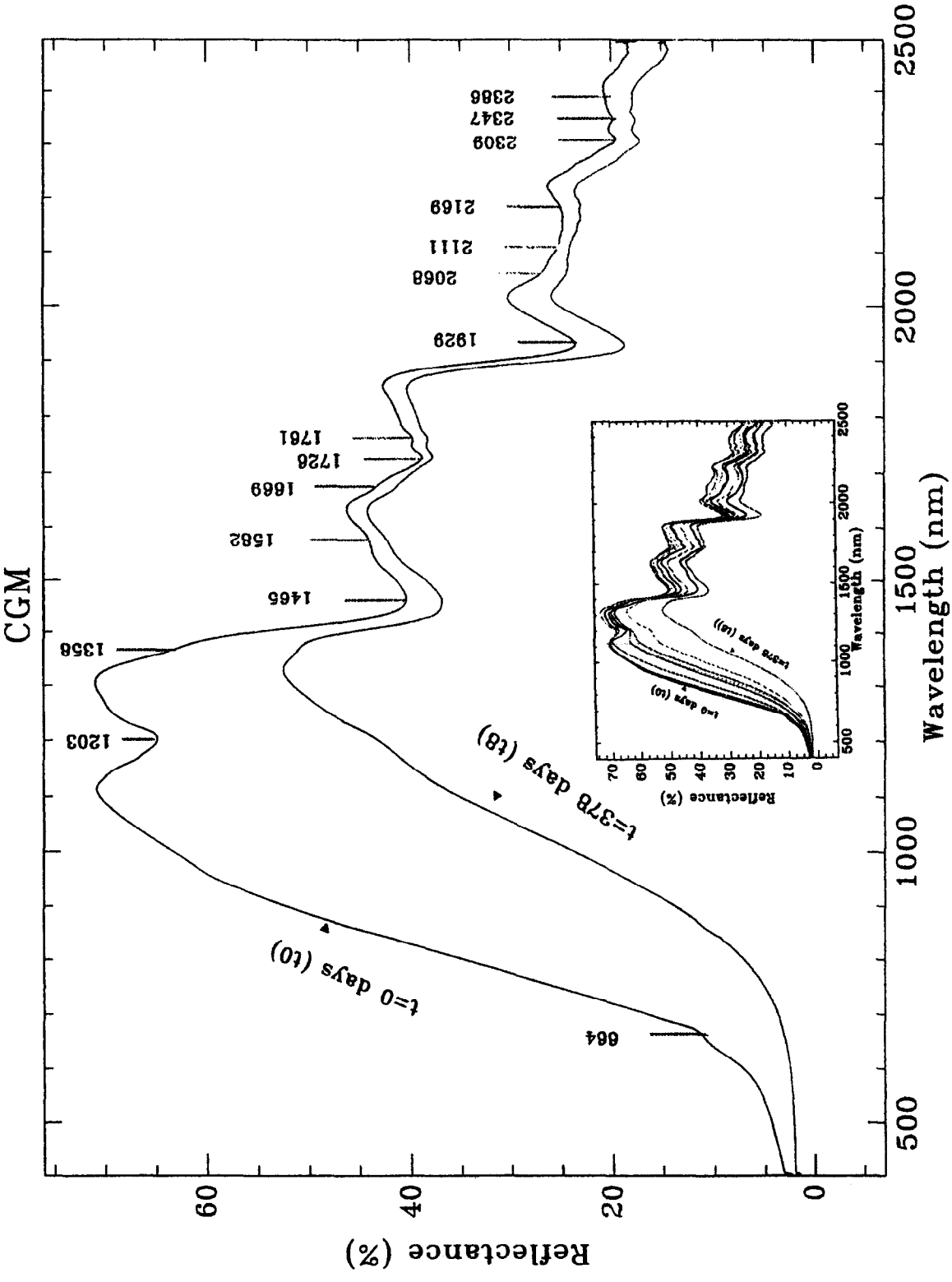

Figure 1. The reflectance spectra of two endnumbers that represent the two extreme composting stages t_0=0 days and t_8=378 days for the CGM. Major wavelengths were extracted manually. The small box shows the spectral of all intermediate decomposition stages.

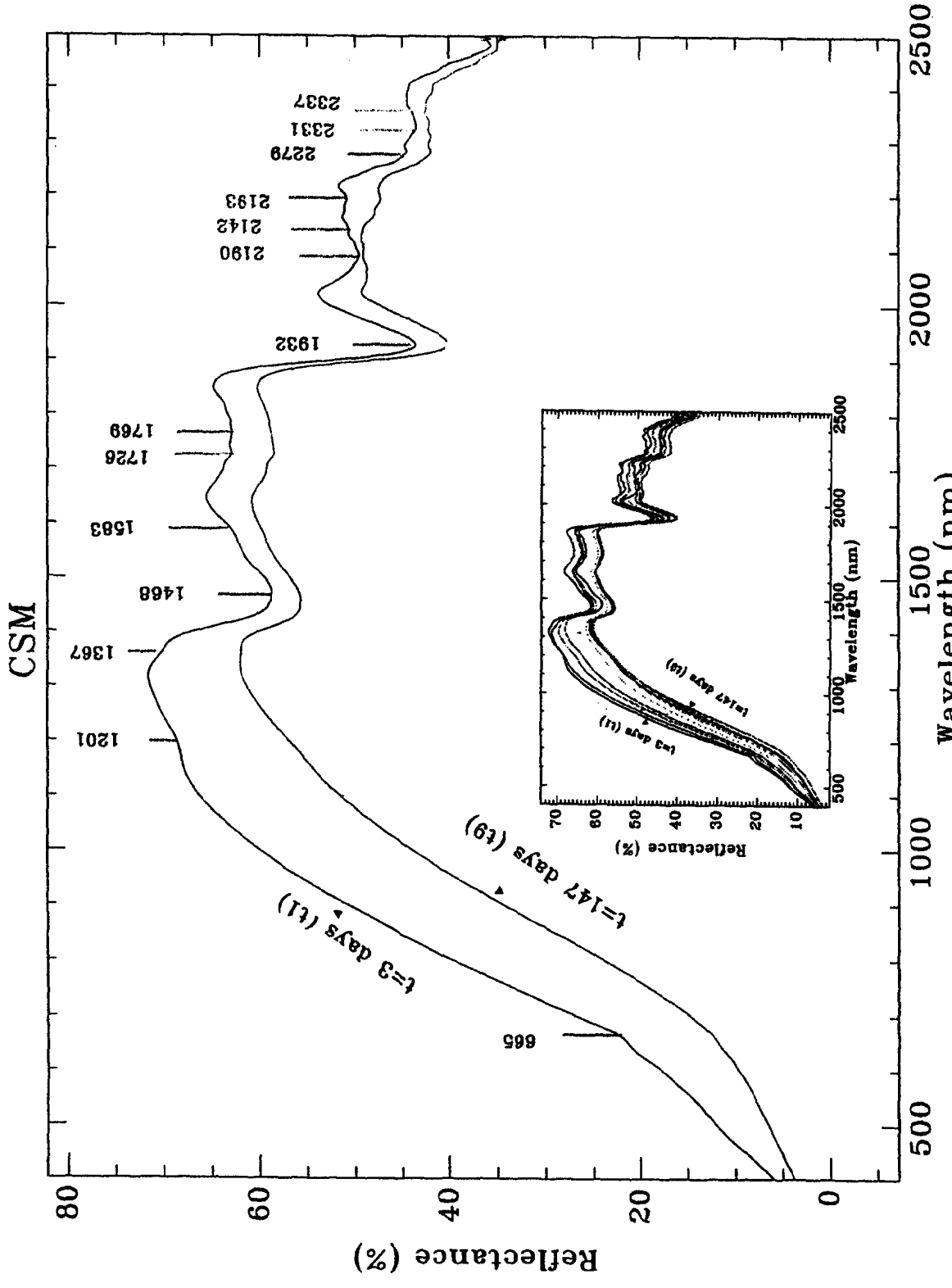

Figure 2. The reflectance spectra of two endmembers that represent the two extreme composting stages $t_1=3$ days and $t_9=147$ days for the CSM. Major wavelengths were extracted manually. The small box shows the spectra of all intermediate decomposition stages.

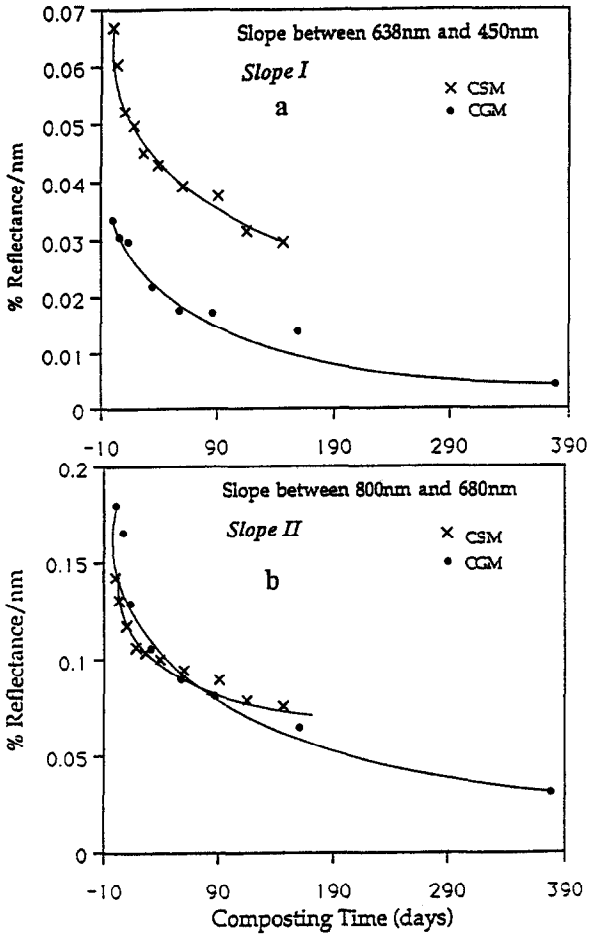

Figure 3. The reflectance slope values between 638 nm and 450 nm [a) slope I] and between 800 nm and 680 nm [b) slope II] plotted against the composting time.

In Figure 3a (slope I), two separate curves representing the CGM and CSM clearly show that an offset of about 0.02 slope units exists between the two curves throughout the entire composting time. In Figure 3b (slope II), however, the two curves appear to overlay each other for all composting stages, and no significant difference can be observed. These findings strongly suggest that slope II is less sensitive to the compost (organic matter) species than slope I, and thus may be used as a general parameter for monitoring organic matter maturity. Likewise, slope I is a more sensitive parameter for identifying compost (or organic matter) species, and hence may be used as a parameter for identifying both the degradation condition and the parent material status of the organic matter. Judging from the rapidly decreasing rate of both slopes (I and II) during the first decomposition stage (0–60 days) in the controlled process, it is evident that a precaution must be taken in assessing organic matter content using slope (or ratio and albedo) parameters based on the visible region during the first stage of organic matter degradation (note that in the soil-field process this period may be even longer). For instance, Krishnan et al. (1980), pointed out that the slope of the soil reflectance curve near 800 nm increases with organic matter content in soil. As discussed previously, the reflectance slope between 800 nm and 680 nm (slope II) is strongly dependent upon the maturity of the organic matter and, hence, Krishnan et al.'s conclusion may be biased if the related organic matter is in its young stage of degradation. Because the spectral regions of both slopes are well covered by most of the remote sensors, and because band rationing is a common technique used to classify objects from such sensors, a precaution regarding this issue must be taken in every organic matter assessment.

Changes in the Spectral Features

From Figures 1 and 2 it can be observed that in the VIS-NIR-SWIR region there are changes in the spectral features (position and intensity) that, in some cases, are easy to detect (e.g., the 1203 nm and 1201 nm in CGM and CSM, respectively) and in others, are difficult to assess (e.g., the 2347 nm and 2279 nm in CGM and CSM, respectively). The spectral features in the NIR-SWIR region are the result of overtones and combination modes of functional groups' fundamentals. Because the chemistry of compost materials (and organic matter as well) at any decomposition stage is thought to be very complex (Inbar et al., 1990; Chen and Inbar, 1994), the corresponding spectrum is rather complex as well. The relatively numerous spectral features, which can be observed in both materials at any stage, suggest that the reflectance spectra consist of important chemical information. It is interesting to note, however, that general similarities exist between the two fresh materials' spectra (t_0 and t_1 for CGM and CSM, respectively) and the spectra of fresh (and dry) oak leaves given by Gao and Goetz (1994) and dry brown leaves given by Elvidge (1990). This suggests that, although organic matter is thought to be very complex material, it may be categorized in representative spectral groups. Further work in order to fully understand this phenomenon is still required but was beyond the scope of this article.

The major absorption peaks, as directly extracted from Figures 1 and 2, and their possible spectral assignments are given in Tables 2 and 3, for CGM and CSM, respectively. As shown by Elvidge (1990), absorption features of major and pure organic matter components (e.g., cellulose, lignin, starch, pectin, and wax) may overlap across the NIR spectral region making their assignments a rather complicated task. As a result, we based our assignments on direct calculation of the overtones and combination modes of well-assigned features from the IR region and on the chemical information for the exact population that was reported by both Inbar et al. (1991; 1992) and Chen and Inbar (1994). Additionally, we also attributed possible components associated with the chemical groups identified by other workers.

Table 2. Suggested CGM Assignments for the Major Absorption Features Extracted from Figure 1 at t_0

CGM Wavelength (nm)	*Assignments*[a]	*Possible Components*[b]
664		Chlorophyll pigment
1203		Oil/cellulose/wax
1358	OH in water	Cellulose/lignin/starch
1465	OH in water ($\upsilon_2 + \upsilon_3$); CH_2	Cellulose/lignin/starch/pectin
1582	OH in water (2υ); H-bonded OH group	Pectin/starch/cellulose
1669	2υ aromatic C—H stretch	
1726	2υ of aliphatic C—H stretch	Cellulose/lignin/starch/pectin/wax/humic acid
1761	2υ of aliphatic C—H stretch	Cellulose/lignin/starch/pectin/wax/humic acid
1929	OH in water ($\upsilon_1 + \upsilon_3$); 3υ of —C=O and of —COOH, C=O of ketonic carbonyl, $CONH_2$	Cellulose/lignin/glucan/starch/pectin/wax/humic acid
2068	3υ of aromatic C=C, COO—hydrogen bond, C=O	Cellulose/glucan/pectin
2111	3υ of aromatic C=C, COO—hydrogen bond, C=O	Cellulose/glucan/pectin
2169	3υ of aromatic C=C	Starch/lignin/wax/tannins
2309	3υ of aliphatic C—H, aromatic ring stretch	Humic acid/wax/starch
2347	3υ of aliphatic C—H	Cellulose/lignin/glucan
2386	3υ of COO—, CH_3	Pectin/protein

[a] Calculated from well-assigned IR features of the exact population.
[b] Taken from Elvidge (1990), Curran et al. (1992), and McLellan (1991a,b).

The absorption at around 664 nm in both CGM and CSM materials is attributed to pigment residuals such as chlorophyll. Because chlorophyll pigments are thought to decompose rapidly with time, only weak absorption features could be observed in both materials for the young stages (t_0 and t_1) at around 664 nm, and no absorption features could be found for the mature stages (t_8 and t_9) in CGM and CSM, respectively.

At around 1200 nm, a significant absorption feature is observed for both materials, but it is relatively more intense in the CGM. Absorption in this wavelength exists in cellulose, lignin, wax, and oil, as reported by Elvidge (1990) and Williams and Norris (1987). In the CGM we were more likely to attribute this absorption feature to oil, because the fresh CGM materials contain large portions of grape seeds, which are rich with "oil" (Inbar et al., 1991; 1992). The significant diminishing of the 1203 nm features over time can be explained by the decomposition process, which changes the initial compounds ("oil") into complex substances ("humus"), just as happens with chlorophyll. In the CSM, however, this absorption may be attributed to cellulose, which also decays in a biogenic process very similar to that of the oil and chlorophyll components.

The strong spectral features at around 1460 nm and 1930 nm are attributed to the combination modes of OH in water molecules. Since the materials were air-dried prior to the spectral measurements, we assume that the water molecules are all in the adsorbed position on the organic matter's surfaces. At this stage, however, no reasonable sequence can be identified between the spectral parameter (e.g., spectral depth) and the composition time. It should be noted, however, that the water feature around 1460 nm may overlaps with other OH groups in cellulose molecules (Elvidge 1990) or with CH_2 groups in lignin molecules (McLellan et al., 1991a), and, thus, accurate assignment of this feature may be difficult.

The weak spectral feature at around 1360 nm may

Table 3. Suggested CSM Assignments for the Major Absorption Features Extracted from Figures 2 at t_1

CSM Wavelength (nm)	*Assignments*[a]	*Possible Components*[b]
665		Chlorophyll pigment
1201		Oil
1367	OH in water	Cellulose/lignin/starch
1468	OH in water ($\upsilon_2 + \upsilon_3$)	Cellulose/lignin/starch/pectin
1583	OH in water ($2\upsilon_1$); H-bonded OH group	Pectin/starch/cellulose
1726	2υ of aliphatic C—H stretch	
1769	2υ of aliphatic C—H stretch	Cellulose/lignin/starch
1932	H_2O ($\upsilon_1 + \upsilon_3$); 3υ of —C=O and of COOH, C=O of ketonic carbonyl, $CONH_2$	Cellulose/lignin/glucan/starch/pectin/humic acid
2142	3υ of C=C of aromatic rings	Starch/lignin/wax/tannins
2193	Amid II	Protein
2279	3υ of CH_2, CH_3	
2331	3υ of CH_2, COO—	Cellulose/lignin/glucan
2337	3υ of COO—, CH_3	Pectin/protein

[a] Calculated from well-assigned IR features of the exact population.
[b] Taken from Elvidge (1990), Curran et al. (1992), and McLellan (1991a,b).

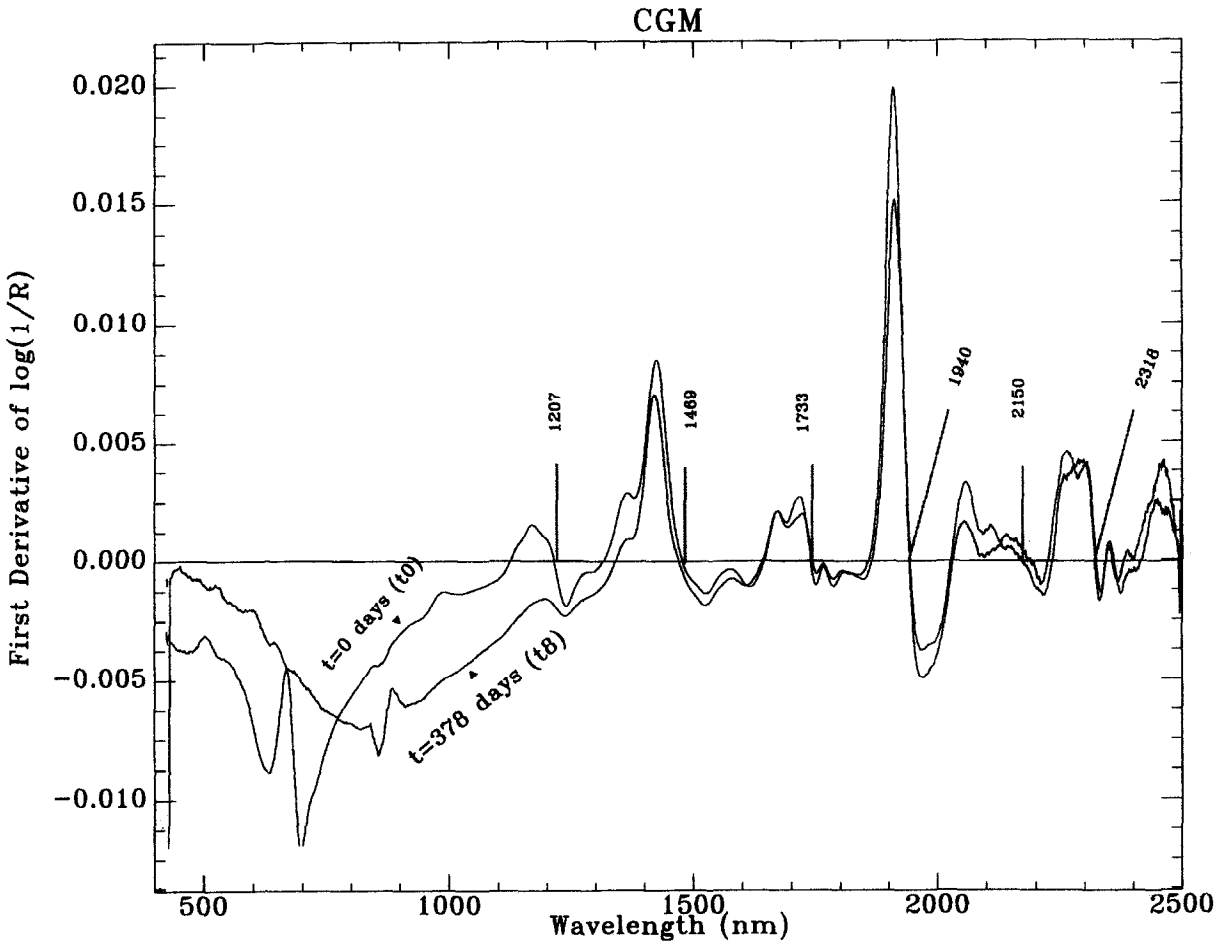

Figure 4. The first derivative spectra of the two endmembers presented in Figure 1 for CGM.

be attributed to OH molecules in free water or in cellulose/lignin/starch, and the weak feature at 1583 nm to H-bonded OH groups in water molecules. The relatively weak, but significant, spectral features across the NIR-SWIR region (1100–2500 nm) may be assigned to functional groups associated with C—H, C=O, C=C, and —COOH in various configurations (aromatic or aliphatic) and other groups such as —CO—NH_2. Second and third overtones of the above fundamentals can be used to explain most of the wavelengths' positions. In both CGM and CSM materials, three basic regions, beyond 1300 nm can be defined: at around 1400–2000 nm, around 2100–2200 nm, and around 2100–2250 nm.

Spectral Manipulations

Practically it is difficult to visually extract and effectively monitor spectral changes directly from the raw reflectance spectra. Consequently, we applied several manipulation techniques to the raw spectra in order to enhance and assign maximum spectral information (strong and weak). The spectral manipulations included: conversion of the raw reflectance data (R) into apparent absorption (A) [$A=\log(1/R)$], first derivative of A (A') and second derivative of A (A''). In Figures 4 and 5, the first derivatives of the absorption spectra $\{A'=[\log(1/R)]'\}$ in the two selected endmembers are presented for the CGM (t_0 and t_8) and the CSM (t_1 and t_9) materials, respectively. Theoretically, the first derivation technique manipulates a Gaussian-like peak as a doubletlike feature that crosses the X-axis at the original maximum position (Owen, 1987; Hruschka, 1987). From Figures 4 and 5 it can be seen that several doubletlike peaks occur in the SWIR region (1300–2500 nm) but not in the VIS-NIR region (400–1200 nm). In the VIS region the first derivative does not fully correct the "baseline shift" since the original VIS spectra have steep slopes. As a result, the doublets at around 665 nm and 1202 nm do not cross the X-axis at zero and thus allocate under negative Y values. Besides correcting the baseline effects in the SWIR region, note that the A' manipulation also enhances some of the weak spectral features throughout the entire spectral region. Consequently, it enables better observation of spectral changes occurring from one composting stage to another. For example, compare the chlorophyll absorption changes at 665 nm in the R and A' spectra for both materials (Figs. 1 and 2 to Figs. 4 and 5, respec-

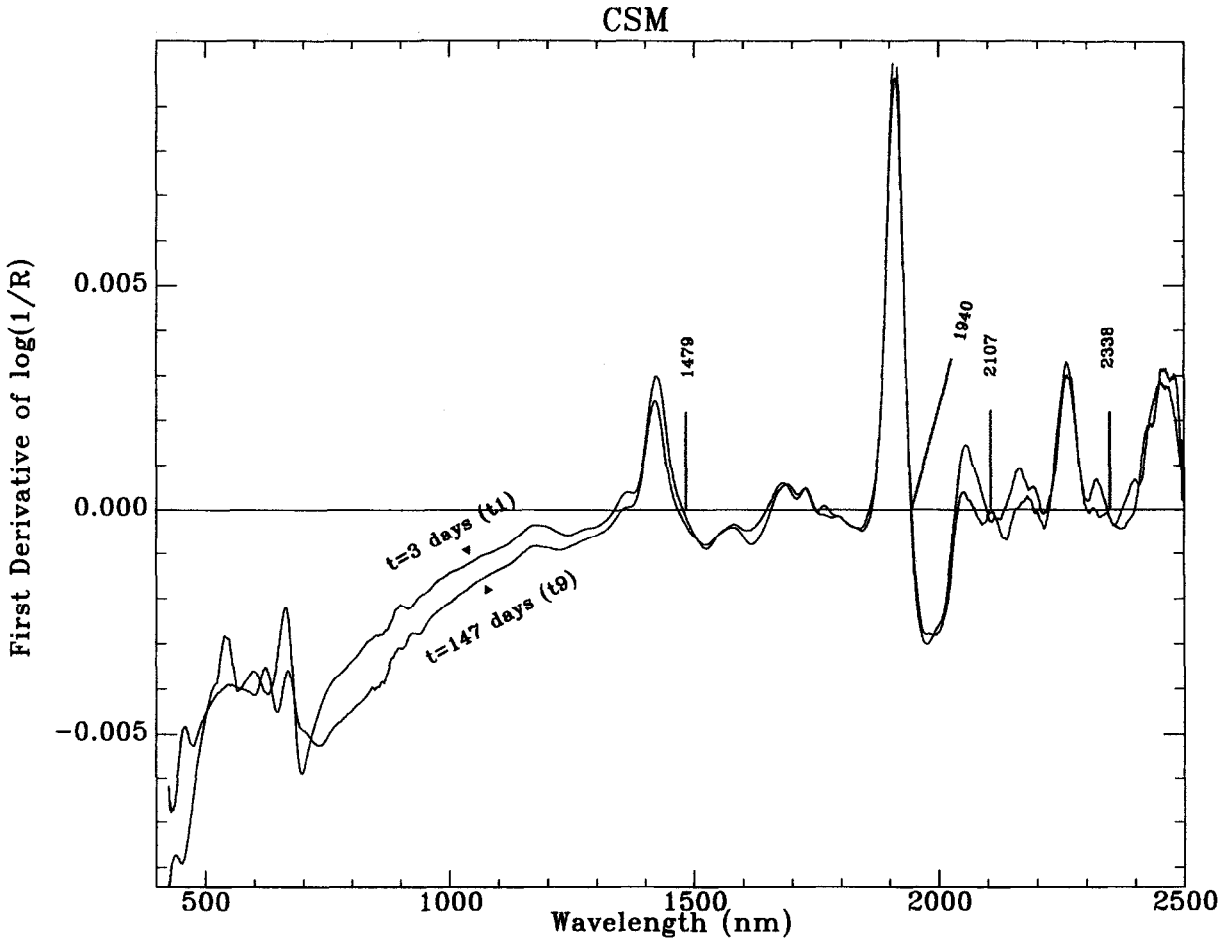

Figure 5. The first derivative spectra of the two endmembers presented in Figure 2 for CSM.

tively). It is evident that, in the original R spectra, the spectral feature is rather weak and in the A' spectra is significantly enhanced. Moreover, the derivation technique enables easy detection of the exact position of the original R peak by using the "crossing X-axis" point in the first derivative spectra. Using this tool, it is evident that a significant spectral shift occurred at around 1400 nm for both materials [the 1469 nm and 1479 nm peaks in the young stage were shifted to 1415 nm and 1430 nm in the mature stage for the CGM and CSM, respectively (Figs. 4 and 5)], while no equivalent changes could be detected for the second water peak at 1940 nm. Careful observation of decomposed *Quercus alba* foliage's spectra that were given by McLellan et al. (1991a) reveal a similar "visible" shift of the 1450 nm band. This suggests that the band shift at around 1400 nm is not an occasion event but has a physical base meaning. Since McLellan's samples were oven dried prior to the spectral measurements, it is assumed that such a shift more likely occurred because of OH bond changes in the cellulose/lignin component or perhaps to the CH_2 groups rather than OH in the free water molecules. However, to fully examine this assumption, more study is required.

Figures 6 and 7 present the second derivation of the absorbance spectra [$A''=\log(1R)''$] for both previous endmembers. It can be clearly seen that most of the spectral variations fluctuate around the X-axis and that the "baseline shift" effect (which mostly occurs in the VIS region) has been totally removed. Because the second derivative technique actually doubles the correction of the "baseline" effect, the above observation is expected. Also notice that the A'' spectra better enhances very small weak spectral features that were hardly observed in the original R spectra. To better judge this improvement, we plotted in Figures 8 and 9 the original R spectra of t_0 and t_1, for CGM and CSM, respectively, together with their corresponding A'' spectra. Careful observation of both figures reveals an interesting finding as follows: The second derivative of the A'' spectra is actually a simple exaggeration of the original R spectra (see, e.g., the R shoulder at 1950 nm that turned into a strong feature in the A'' mode and a similar trend for the weak chlorophyll feature at 665 nm). Each of the features in the R-space holds a similar position in the A'' space (which technically slightly shifted toward the VIS region due to the derivation process). A second derivation of any Gaussian

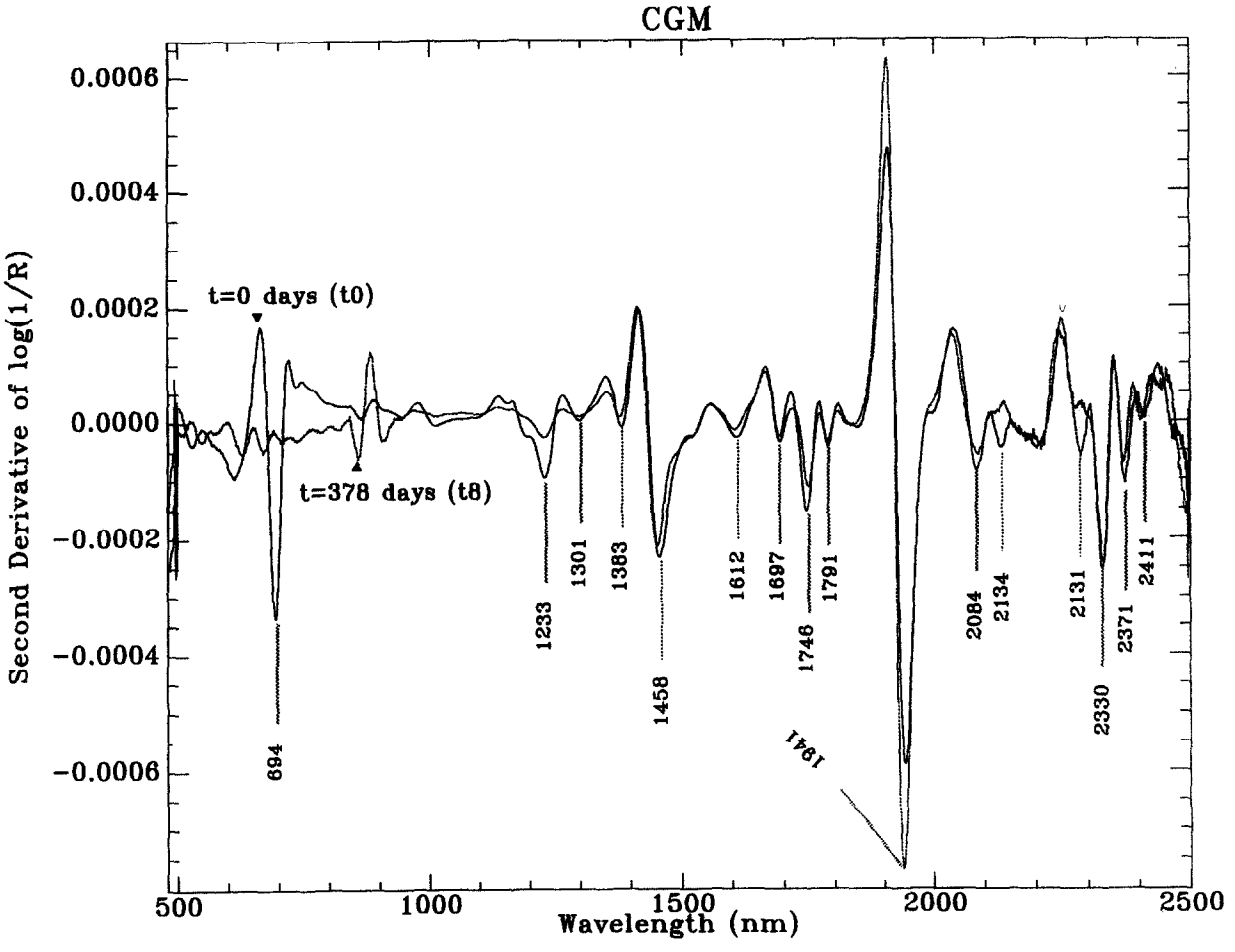

Figure 6. The second derivative spectra of the two endmembers presented in Figure 1 for CGM.

peak reveals that the middle portion of the derivatives is curved downward (Hurschka, 1987). Thus, transformation of the reflectance (R) spectrum into absorbance (A), which produces an inverse R presentation, and then taking its derivative it twice (A'') actually reyields the R peak's position again, but with a significant enhancement. Although the above mechanism is widely understood (e.g., Williams and Norris, 1987; Norris and Williams, 1984), traditionally workers prefer to present the original spectrum with its derivatives rather than plot the original spectrum with its manipulated derivatives, that is, A with A' (or A'') and R with R' (or R'') rather than R with A' (or A''). Consequently, such a phenomenon could not be fully considered and described elsewhere.

Spectral Analysis

In this section we applied the near-infrared analysis (NIRA) methodology (Davies and Grant, 1987) to the raw and manipulated spectra. In addition to a wide use of the NIRA technique in many disciplines and applications (e.g., food science, textiles, and pharmacology) it has been successfully applied in the field of soil science (Ben-Dor and Banin, 1994) and in soil organic matter issues (Krishnan et al., 1980; Dalal and Henry, 1986; Morra et al., 1991). McLellan et al. (1991a,b) used NIRA to predict the amounts of nitrogen, lignin, and cellulose during a decomposition process of leaf materials and felt that the method has the potential of becoming the standard method for rapid evaluation of the chemical makeup of fresh and decomposed plant materials.

The NIRA path we employed consisted of a linear regression analysis between all of the spectral readings across the spectrum (in the R, A, A', and A'' modes) and their composting times to objectively select the best explained wavelength. Then, a multiple regression analysis (MRA) between the composting time and the highest correlation wavelengths and their spectral readings was run to yield a multiterm equation as follows:

$$C_p = b_0 + b_1L_1 + b_2L_2 + \ldots + b_nL_n \,, \qquad (1)$$

where C_p is the predicted composting time, b_0 is an intercept, b_1, b_2, . . ., b_n are weighting factors, and L_1, L_2, . . . , L_n are the spectral readings at wavelengths 1, 2, . . . , n.

This procedure employed four sets of manipulated spectra (R, A, A', and A''). Every spectral reading that

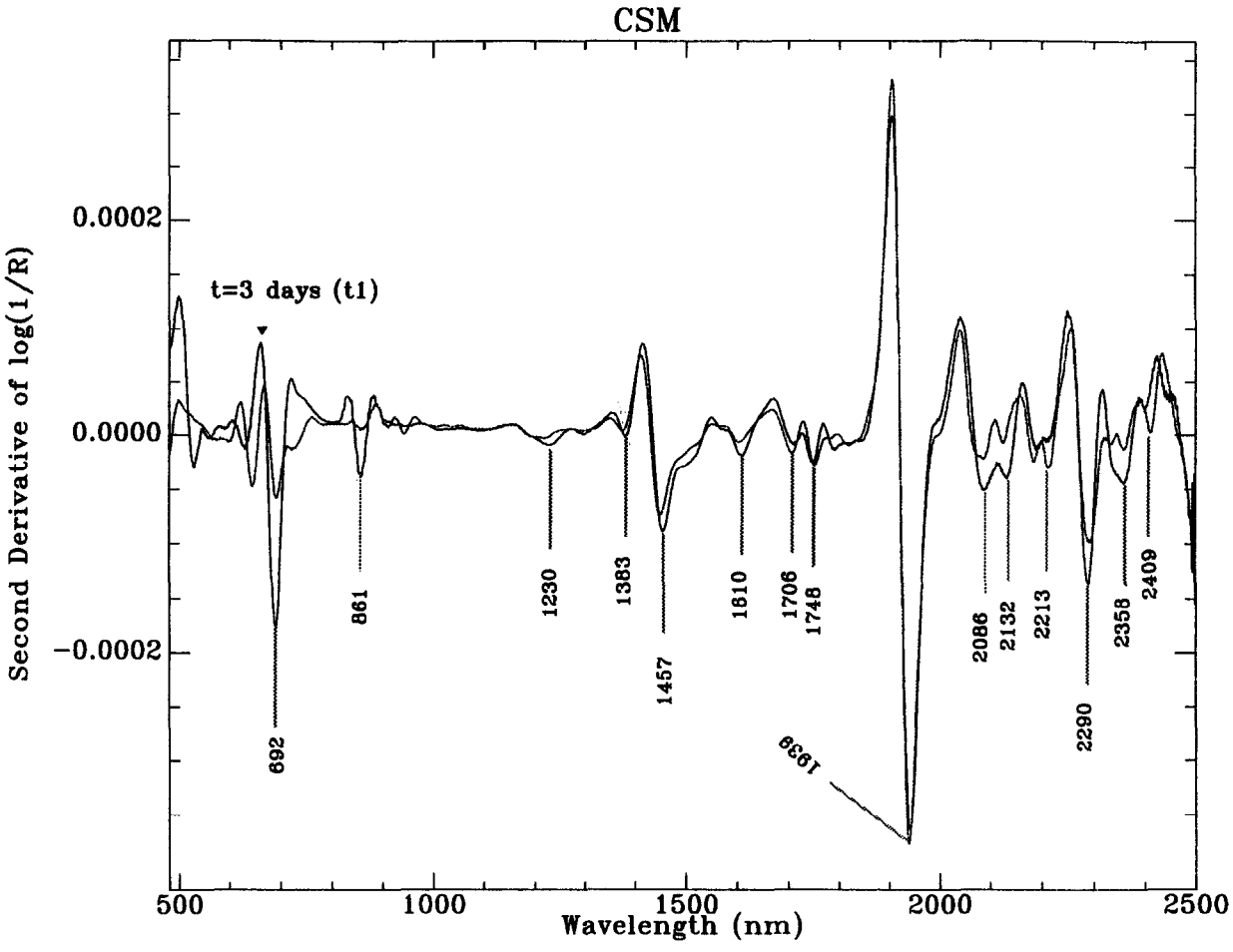

Figure 7. The second derivative spectra of the two endmembers presented in Figure 2 for CSM.

was allocated above a correlation coefficient threshold of $r=\pm 0.90$ in the linear regression analysis was used in the MRA. The standard error of calibration (SEC) that was calculated according to Davies and Grant (1987) is as follows:

$$\text{SEC} = \sqrt{\frac{\sum(C_m - C_p)^2}{N_c - t - 1}}, \qquad (2)$$

where C_m is the original composting time, C_p again is the predicted composting time, t is the number of terms in the MRA equation, and N_c is the number of samples in the analysis.

We selected the above NIRA routine, which has been extensively described and used elsewhere (e.g., Stark and Luchter, 1986) from all other available routines, because it provides good judgment for every step involved in the analysis. This strategy is very important when a new population and system is being examined, as was the case in this study.

The best prediction equations for CGM and the CSM (from all examined) are presented in Table 4, whereas Figures 10a and 10b show the predicted composting time calculated directly from these equations. In both the CGM and CSM series, the first wavelength is attributed to the water molecules as discussed earlier. Inbar et al. (1989) observed that, for the CSM, the spectral peak of the H-bonded OH groups, at 3400 cm^{-1} (associate with υ_1 fundamental of water) decreases as the compost ages, and hence confirms the correlation obtained by the reflectance data (via A'' or A' manipulations).

In the CGM, the first selected wavelength was 1887 mm, and in the CSM it was 1560 nm, which were both associated with water molecules ($\upsilon_2+\upsilon_3$ and $2\upsilon_1$, respectively). The $\upsilon_2+\upsilon_3$ assignment stands in good agreement with Downey and Byrne's 1986 results (Downey and Byrne, 1986), who found that a similar combination was greatly responsible for the moisture assessment in milled peat. As was shown by Elvidge (1990), around 1560 nm both cellulose and pectin materials consist of relatively enhanced features that may be also related to the above OH assignments.

Since the samples were air-dried for the reflectance measurements and consisted of relatively high correlations between hygroscopic moisture and composting time ($r^2=0.81$, data not shown), this wavelength strengthens the assumption that the data actually represent hygro-

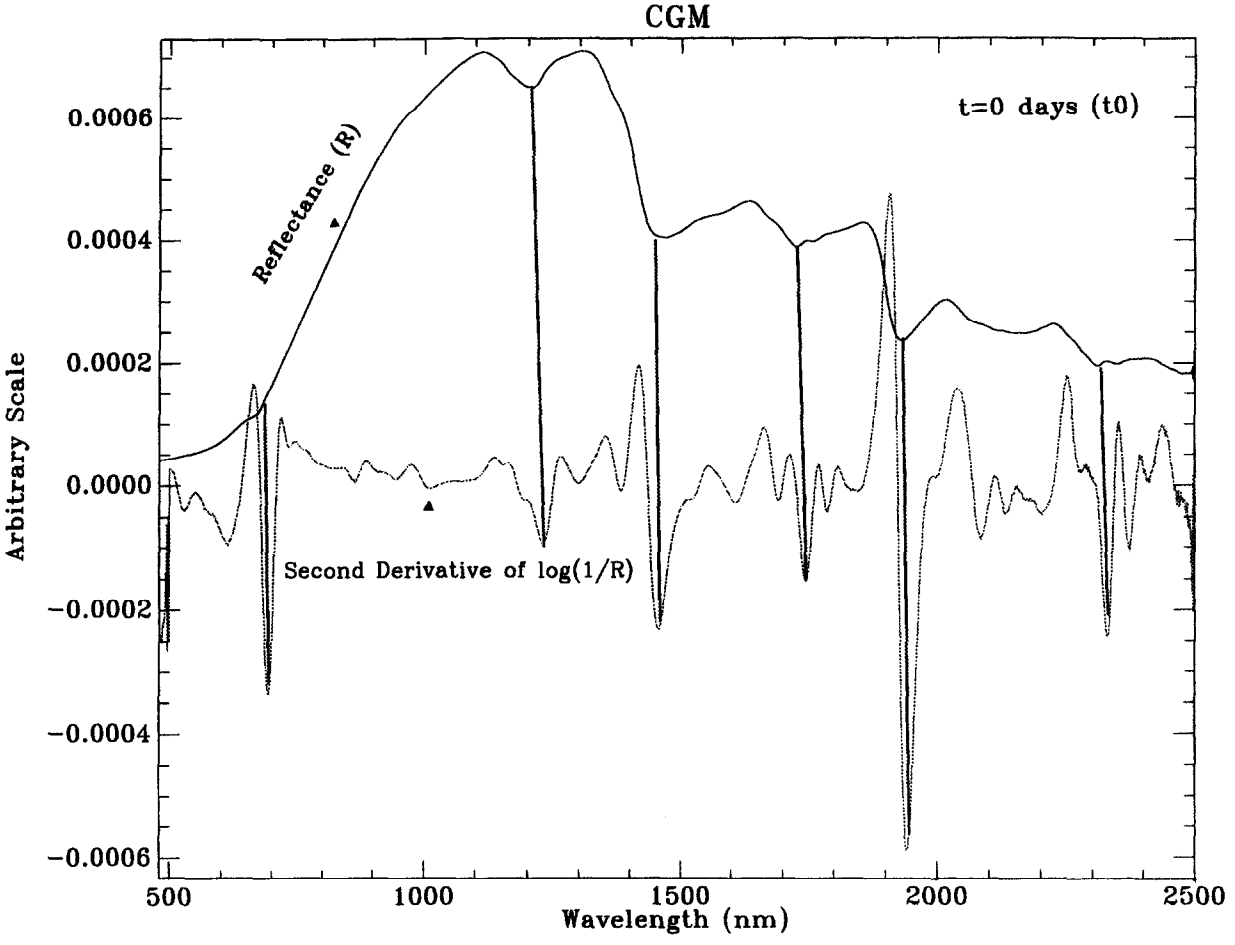

Figure 8. The second derivative spectrum (A'') of CGM (at $t=0$ days) and its original reflectance spectrum (R). For clarity, vertical bars have been drawn to indicate peak positions in both spectra.

scopic moisture. It is important to note, however, that such a relationship requires that the measured sample will be in a state of equilibrium with the water vapor prior to the spectral measurement. This is because the adsorbed (and not the free) water is highly correlated with the specific surface area (SSA). For both CGM and CSM, Inbar et al. (1989; 1994), pointed out that the cation exchange capacity (CEC) increases in a saturation-like function with composting time. Since SSA and CEC are correlated with each other, we expect that the SSA of the mature compost is also relatively high and, hence, is responsible for the significant correlation with the surface adsorbed (hygroscopic) water. This suggests that a cocorrelation between hygroscopic water and pure materials such as cellulose may exist. Other wavelength assignments may be associated with starch at 1370 nm [for CSM, based on Curran et al. (1992)] with aliphatic C—H at 1725 nm (for CGM) and with protein and lignin at 2351 nm for CSM, based on Elvidge (1990). It should be noted at this point that the number of samples used for each material was still rather low for significant NIRA analysis (Murray, 1988). As a result, we could not provide an independent validation examination for each of the equations and, consequently, assumed that if a reasonable number of samples existed, other MRA equations could be generated and different wavelengths and weighing factors could be obtained. We therefore strongly recommend that further study be applied in similar systems in order to investigate the capability of the reflectance spectra to provide significant prediction equations of the chemistry of unknown samples. Nevertheless, there is no doubt that the reflectance properties provided invaluable information regarding aging conditions of organic matter.

SUMMARY AND CONCLUSIONS

The reflectance spectra of compost material in the VIS-NIR-SWIR spectral region consist of invaluable information. In the VIS-NIR region the information is more related to the baseline shape (color), while in the NIR-SWIR region the information is more related to the specific absorption features. Use of a spectral derivation technique enhanced weak spectral features and extracted

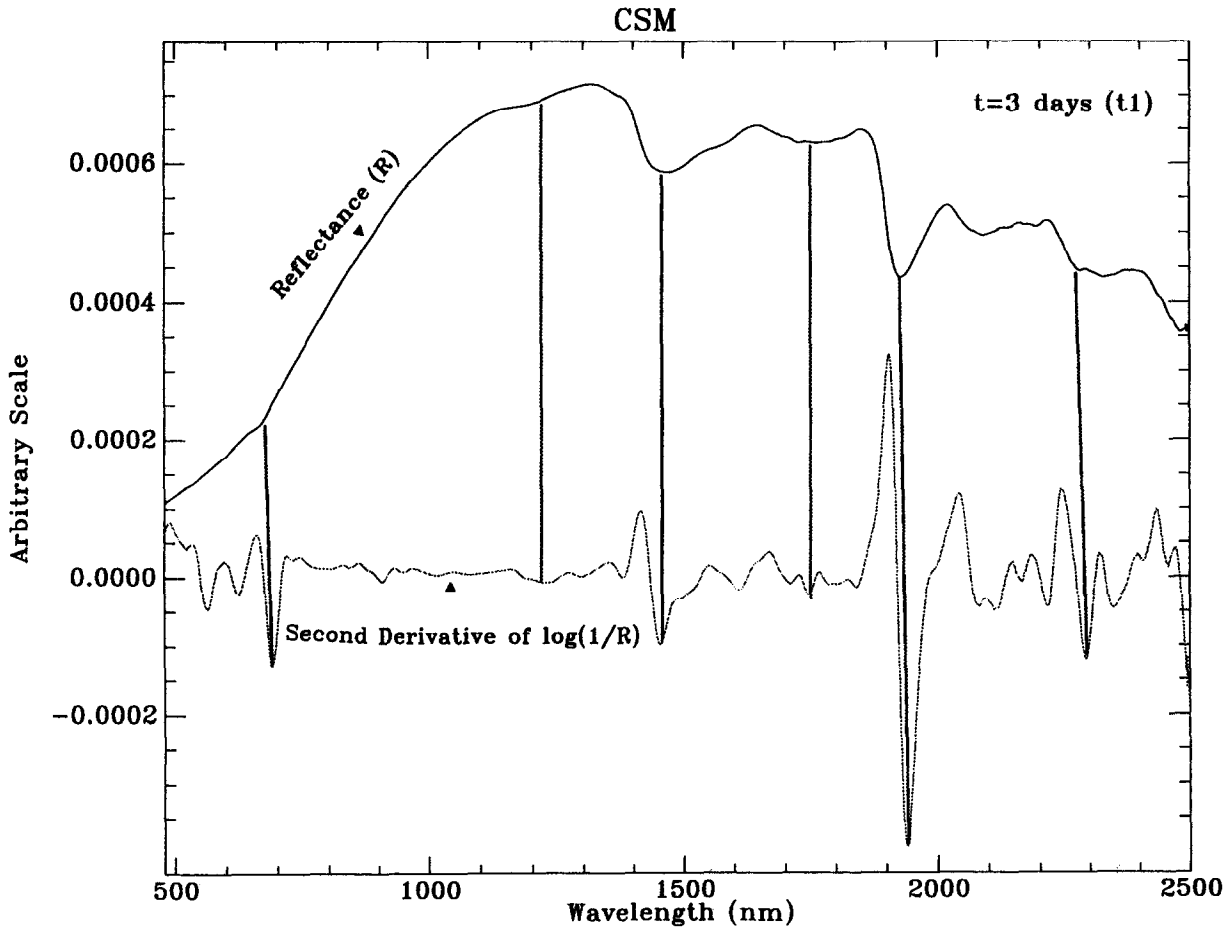

Figure 9. The second derivative spectrum (A'') of CSM (at t=3 days) and its original reflectance spectrum (R). For clarity, vertical bars have been drawn to indicate peak positions in both spectra.

hidden information. The slope values in the visible region were found to be a significant parameter for monitoring the compost maturity with and without relying on the organic matter species (638 nm/450 nm and 800 nm/680 nm, respectively). We assumed that these parameters are strongly controlled by the intense ultraviolet absorption of components such as lignin, tannins, and pectin. Since similar parameters can be derived by most of the remote sensing equipment, it is speculated that such parameters could also be used to monitor organic matter conditions from orbit. In addition, it is assumed that organic matter assessments using VIS slope (or ratio) parameters are highly likely to be biased by the stage of maturity of the organic matter in the field, and hence, if not used properly, could provide errors in the organic matter assessment. Spectral derivation enhanced hidden information such as a significant spectral shift at 1450 nm with aging and detection of small spectral changes. Multiple regression analysis was found to yield reasonable equations for explaining most of the variations observed in compost aging. The OH and aliphatic C—H groups combined with water, cellulose, starch, pectin, and pro-

Table 4. The Optimal Calibration Equation Selected for Predicting Compost Time from the Reflectance Measurements and Suggested Assignments for the Included Wavelengths

Material	*Manipulation*	*SEC*[a] *[r^2]*	*Constant*	*Weighting Coefficient*	*Wavelength (nm)*	*Assignment, Materials*
CGM	A'	12.38 [0.988]	−587.15	7273.6	1887	OH, water
				5682.7	1725	C—H, starch/cellulose
CSM	A''	3.06 [0.994]	−48.24	26,616	1560	OH, water
				71,777	1370	OH, water/cellulose/starch
				8005	2351	Lignin/protein

[a] See text for definition. Values in days.

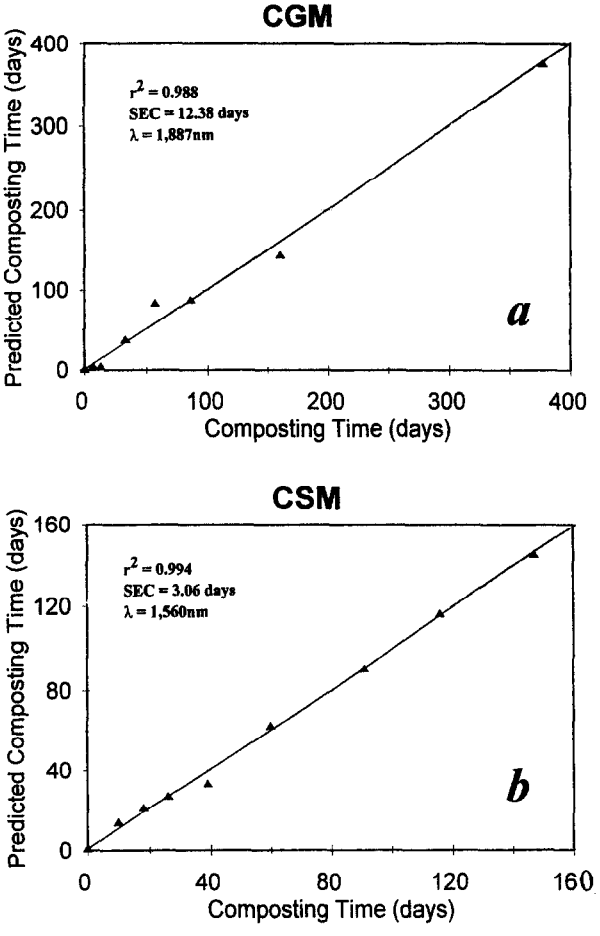

Figure 10. The predicted composting time as calculated using the best MRA equation values against the composting time in a) CGM and b) CSM.

tein molecules were found to be the components that best correlated with the composting time. Although similar analysis has not been carried out for other compost properties, it is strongly believed that an interrelation between composting time and compost chemistry will yield similar (or even better) results. More samples require analysis in order to establish a general multiterm equation for predicting unknown compost samples. It can be concluded that the VIS-NIR-SWIR spectra is not only a promising tool for monitoring the composting process in a real time mode, but also a valid technique in which important and new information about aging organic matter can be retrieved and used in the remote sensing field. Another important conclusion is that the composting process may prove to be a valid tool for creating spectral libraries in a relatively short time frame.

This article is in memory of Mr. A. T. Shapiro, who was a programmer at The Center for the Study of Earth from Space, University of Colorado at Boulder, and was involved with the statistic analysis portion. Mr. Shapiro's assistantship in this study and many others played a major role in our scientific activity at CSES. Some of the studies he assisted with were published during the years 1993–1996.

REFERENCES

Aber, D. J., Wessman, C. A., Peterson, S. L., Melillo, J. M., and Fownes, J. H. (1990), Remote sensing of litter and soil organic matter decomposition in forest ecosystems, in *Remote Sensing of Biosphere Functioning* (R. J. Hobbs, H. A. Mooney, Eds.) Springer-Verlag, New York, pp. 87–101.

Al-Abbas, A. H., Swain, P. H., and Baumgardner, M. F. (1972), Relating organic matter and clay content to the mutispectral radiance of soils. *Soil Sci.* 114:477–485.

Ben-Dor, E., and Banin, A. (1994), Visible and near infrared (0.4–1.1 μm) analysis of arid and semiarid soils. *Remote Sens. Environ.* 48:261–274.

Ben-Dor, E., and Kruse, F. A. (1995), Surface mineral mapping of Makhtesh Ramon Negev Israel using 63 channel scanner data. *Int. J. Remote Sens.* 16:3529–3553.

Boardman, J. W., and Kurse F. A. (1994), Automated spectral analysis: a geological example using AVIRS data. North Grapevine Mountains, Nevada. In *Proceedings of the Tenth Thematic Conference on Geological Remote Sensing*, San Antonio, TX, Vol. I, pp. 407–418.

Buol, S. W., Hole, F. D., and McCracken, R. J. (1973), *Soil Genesis and Classification*, Iowa State University Press, Ames, 360 pp.

Chang, S. H., Sorensen, B. M., and Rubin, T. D. (1994), A general purpose scanner for airborne remote sensing, in *Proceedings of the First International Airborne Remote Sensing Conference and Exhibition*, Strasbourg, France, Vol. II, pp. 155–158.

Chen, Y., and Inbar, Y. (1994), Chemical and spectroscopic analysis of organic matter transformations during composting in relation to compost maturity. In *Science and Engineering of Composting* (A. J. Hoitink and H. M. Keener, Eds.), Renaissance Publication, Worthington, OH, pp. 551–600.

Curran, P. J., Dungan, J. L., Macler, B. A., Plummer, S. E., and Peterson, D. L. (1992), Reflectance spectroscopy of fresh whole leaves for the estimation of chemical concentration. *Remote Sens. Environ.* 39:153–166.

Dalal, R. C., and Henry, R. J. (1986), Simultaneous determination of moisture organic carbon and total nitrogen by near infrared reflectance spectrophotometery. *Soil Sci. Soc. Am. J.* 50:120–123.

Davies, A. M. C., and Grant, A. (1987), Review: near infrared analysis of food. *Int. J. Food Sci. Technol.* 22:191–207.

Downey, G., and Byrne, P. (1986), Prediction of moisture and bulk density in milled peat by near infrared reflectance. *J. Food Sci. Agric.* 37:231–238.

Elvidge, C. D. (1990), Visible and near infrared reflectance characteristics of dry plant materials. *Int. J. Remote Sens.* 11:1775–1795.

Gao, B. C., and Goetz, F. A. H. (1994), Extraction of dry leaf spectral features from reflectance spectra of green vegetation. *Remote Sens. Environ.* 47:369–374.

Grove, C. I., Hook, S. J., and Palor, E. D., II (1992), Laboratory reflectance spectra of 160 minerals, 0.4–2.5 microme-

ters, JPL Publication 92-2, Jet Propulsion Laboratory, Pasadena, CA, 356 pp.

Hruschka, W. R. (1987), Data analysis: wavelength selection methods. In *Near Infrared Technology in the Agricultural and Food Industries* (P. C. Williams and K. H. Norris, Eds.), American Association of Cereal Chemists, St. Paul, MN, pp. 35–57.

Inbar, Y., Chen, Y., and Hadar, Y. (1988), Composting of agriculture wastes for their use as container media: simulation of the composting process. *Biol. Wastes.* 26:247–259.

Inbar, Y., Chen, Y., and Hadar, Y. (1989), Solid-state carbon-13 nuclear magnetic resonance and infrared spectroscopy of compost organic matter. *Soil Sci. Soc. Am. J.* 53:1695–1701.

Inbar, Y., Chen, Y., and Hadar, Y. (1990), Humic substances formed during the composting of organic matter. *Soil Sci. Soc. Am. J.* 54:1316–1323.

Inbar, Y., Chen, Y., and Hadar, Y. (1991), Carbon-13 CPMAS NMR and FTIR spectroscopic analysis of organic transformation during composting of solid wastes from wineries. *Soil Sci.* 152:272–282.

Inbar, Y., Hadar, Y., and Chen, Y. (1992), Characterization of humic substances formed during the composting of solid wastes from wineries. *Sci. Total Environ.* 113:35–48.

Inbar, Y., Chen, Y., and Hoitnik, H. A. J. (1994), Properties for establishing standards for utilization of composts in container media. In *Science and Engineering of Composting.* (A. J. Hoitink and H. M. Keener, Eds.), Renaissance Publications, Northington, OH, pp. 668–694.

Krishnan, P., Alexander, J. D., Butler, B. J., and Hummel, J. W. (1980), Reflectance technique for predicting soil organic matter. *Soil Sci. Soc. Am. J.* 44:1282–1285.

Krishnan, P., Bulter, B. J., and Hummel, J. (1981), Close-range sensing of soil organic matter. *Trans. ASAE 79–1505*: 306–311.

Kristof, S. J., Baumgardner, M. F., and Johannsen, C. J. (1971), Spectral mapping of soil organic matter. In *Proceedings of the American Society of Agronomy Meetings,* Tucson, AZ pp. 479–489.

Kruse, F. A., and Hauff, P. L. Eds. (1992), *The IGCP-264 Spectral Properties Database,* internal publication, Center for the Study the Earth from Space, University of Colorado, Boulder, 210 pp.

Leger, R. G., Millette, G. J. F., and Chomchan, S. (1979), The effects of organic matter, iron oxides and moisture on the color of two agricultural soils of Quebec. *Can. J. Soil. Sci.* 59:191–202.

McLellan, T. M., Aber, J. D., Martin, M. E., Melillo, J. M., and Nadelhoffer, K. J. (1991a), Determination of nitrogen, and cellulose content of decomposing leaf material by near infrared reflectance spectroscopy. *Can. J. For. Res.* 21: 1684–1688.

McLellan, T. M., Aber, J. D., Martin, M. E., Melillo, J. M., Nadelhoffer, K. J. and Dewey, B. (1991b), Comparison of wet chemistry and near infrared reflectance measurements of carbon-fraction chemistry and nitrogen concentration of forest foliage. *Can. J. For. Res.* 21:1689–1693.

Morra, M. J., Hall, M. H., and Freeborn, L. L. (1991), Carbon and nitrogen analysis of soil fractions using near infrared reflectance spectroscopy. *Soil Sci. Soc. Am. J.* 55:288–291.

Munsel Color (1975), *Munsel Soil Color Charts,* MacBeth Division, Kollmorgen, Baltimore.

Murray, I. (1988), Description of NIR spectra in terms of X-H chromophores. In *Analytical Applications of Spectroscopy* (C. S. Creaser and M. C. Davies, Eds.), The Royal Society of Chemistry, London, pp. 39–51.

Norris, K. H., and Williams P. C. (1984), Optimization of mathematical treatments of raw near infrared signals in the measurements of protein in hard red spring wheat. I. Influence of particle size. *Cearl Chem.* 61:158–165.

Owen, T. (1987), Advances in UV-VIS spectroscopy: derivative spectroscopy. *Int. Lab.* 4:58–64.

Parton, W. J., Ojima, D. S., Cole, C. V., and Schimel, D. S. (1994), A general model for soil organic matter dynamics: sensitivity to litter chemistry texture and management. Quantitative Modeling of Soil Forming Process, Special Publication 39, *Soil Science Society of America,* pp. 147–167.

Stanich, C. G., and Osterwisch, G. F. (1994), Advanced operational hyperspectral scanners: MIVIS and AHS. In *Proceedings of the First International Airborne Remote Sensing Conference and Exhibition,* Strasbourg, France, Vol. II, pp. 191–204.

Stark, E., and Luchter, K. (1986), Near-infrared analysis (NIRA): a technology for quantitative and qualitative analysis. *Appl. Spectrosc. Rev.* 22(4):335–399.

Stoner, E. R., Baumgardner, M. F., Biehl, L. L., and Robinson, B. F. (1980), Atlas of soil reflectance properties, Research Bulletin 962, Agricultural Experiment Station, Purdue University, West Lafayette, IN, 75 pp.

Vane, G., Green, R. O., Chrien, T. G., Enmark, H. T., Hansen, E. G., and Porter, W. M. (1993), The Airborne Visible/Infrared Imaging Spectrometer (AVIRIS). *Remote Sens. Environ.* 44:127–143.

Vinogradov, B. V. (1981), Remote sensing of the humus content in soils. *Pochvovendeniya.* 11:114–123.

Williams, P. C., and Norris, K. H. (1987), Qualitative applications of near-infrared reflectance spectroscopy. In *Near Infrared Technology in the Agricultural and Food Industries* (P. C. Williams and K. H. Norris, Eds.), American Association of Cereal Chemists, St. Paul, MN, pp. 241–321.

Zucconi, F., and de Bertoldi, M. (1987), Compost specifications for the production and characterization of compost from municipal soil waste. In *Compost Quality and Use* (M. de Bertoldi, M. P. Ferranti, P. L. Hermite, and F. Zucconi, Eds.), Elsevier Applied Science, London.